Biophysical Journal Volume 65 October 1993 1740–1748

Substitution of a Hydrophobic Residue Alters the Conformational Stability of Shaker K^+ Channels during Gating and Assembly

Ken McCormack, Ling Lin, and Fred J. Sigworth
Department of Cellular and Molecular Physiology, Yale University School of Medicine, New Haven, Connecticut 06510 USA

ABSTRACT A leucine residue at position 370 (L370) in 29-4 Shaker K^+ channels resides within two overlapping sequence motifs conserved among most voltage-gated channels: the S4 segment and a leucine heptad repeat. Here we investigate the effects observed upon substitution of L370 with many other uncharged amino acid residues. We find that smaller or more hydrophilic residues produce greater alterations in both activation and inactivation gating than does substitution with other large hydrophobic residues. In addition, subunits containing less conservative substitutions at position 370 are restricted in their assembly with wild-type subunits and are unlikely to form homomultimeric channel complexes. Consistent with the idea that L370 influences the tertiary structure of these channels, the results indicate that L370 undergoes specific hydrophobic interactions during the conformational transitions of gating; similar interactions may take place during the folding, insertion, or assembly of Shaker K^+ channel subunits.

INTRODUCTION

Voltage-dependent Na^+, Ca^{2+}, and K^+ channels belong to an extended gene family, the members of which show common functional and structural features (Noda et al., 1986; Tanabe et al., 1987; Tempel et al., 1987; Butler et al., 1990). K^+-permeant channels appear to be tetrameric (MacKinnon, 1991; Liman et al., 1992), whereas Na^+- and Ca^{2+}-permeant channels have a pseudotetrameric structure, consisting of four homologous domains, each roughly equivalent to a single K^+ channel subunit (Catterall, 1988). All of these channels open or "gate" upon relatively small changes in the membrane potential. The "voltage sensor" has been suggested to reside in the charged residues of the presumed transmembrane S4 segment (see Catterall 1988 for a review) (Fig. 1). Consistent with this idea, mutations of the positively charged residues can alter the voltages at which these channels open, as well as the voltage sensitivity (Stühmer et al., 1989; Papazian et al., 1991; Liman et al., 1991; Logothetis et al., 1992). However, equivalent substitutions of the individual residues result in very different effects.

Recently the gating charge of Shaker (*Sh*) channels, the charge associated with the conformational rearrangements during activation, has been measured (Stühmer et al., 1991; Bezanilla et al., 1991; Schoppa et al., 1992). It appears that there are at least two components to the charge movement and that the total magnitude of this movement is approximately 12 elementary charges (Schoppa et al., 1992). This corresponds to a substantial conformational change whereby the S4 segment would have to move as a whole approximately 3/7 of the "electrical width" of the membrane (there are seven charged S4 residues per subunit). Thus, one expects that the conformational rearrangements undergone during gating may have some features in common with the folding and insertion of membrane segments.

Another segment of K^+ channels, the H5 segment located between segments S5 and S6, appears to determine the main portion of the channel pore (Yool and Schwarz, 1991; Hartmann et al., 1991; Yellen et al., 1991). How S4 movement is transduced into channel opening remains unclear. It has been suggested that the position and structure of a region overlapping the S4 and S5 segments might be dependent on the state of S4 activation for a given subunit and that residues in this region might also be involved in protein interactions between subunits that further influence the conformational structure of *Sh* channels (McCormack et al., 1989). Thus, this region may be involved in allosterically coupling the S4 domain to the pore region. Within this region are found hydrophobic leucine residues in a leucine-heptad or "leucine zipper" motif (Landschulz et al., 1989) that is well conserved in *Sh* family K^+ channel sequences and most voltage-gated Na^+ and Ca^{2+} homology domains. The sequence of the *Sh* S4-leucine heptad region is shown in Fig. 1.

Substitutions of uncharged residues in the heptad repeat region have been observed to result in alterations in the voltage dependence (Auld et al., 1990) as well as the voltage sensitivity of activation (McCormack et al., 1991) that are similar to those produced by substitution of charged S4 residues, indicating that these residues undergo protein interactions that influence channel activation. However, similar substitutions of individual leucine residues produce different effects. In addition, alterations in the inactivation properties resulting from some mutations in this region have suggested the possibility that it may form a portion of the receptor for the inactivation ball receptor and thus the internal mouth of the pore (Isacoff et al., 1991; McCormack et al., 1991). If so,

Received for publication 21 October 1992 and in final form 12 July 1993.

Address reprint requests to Dr. Ken McCormack, Max-Planck-Institut für experimentelle Medizin, Herman-Rein Straße 3, 37075 Göttingen, Germany.

0006-3495/93/10/1740/09 $2.00

FIGURE 1 Deduced amino acid sequence of the *Drosophila Sh* S4 and leucine-heptad repeat regions. Basic residues in S4 are denoted by stars, and leucines in the heptad repeat are in bold type. The proposed transmembrane segments S4 and S5 (Tempel et al., 1987) are illustrated by the bars above the sequence. Substitutions for L370 of G, A, S, C, T, V, P, I, M, F, and Y were carried out as described in Materials and Methods.

this region could physically "gate" the pore. In addition, a role for the heptad repeat region in the assembly of *Sh* channels was previously investigated. However, this study was complicated by the fact that a region of the protein upstream of the heptad repeat and the S4 domain was found to result in the association of truncated subunits with wild-type subunits (McCormack et al., 1991); recent biochemical studies have further isolated this region to residues on the cytoplasmic NH_2 terminus (Li et al., 1992). Thus, the role of residues in the S4 and heptad regions in the assembly of full-length subunits remains unknown.

In order to further investigate the role of one of these conserved leucine residues, we substituted residue 370 (Fig. 1 *A*) in *Sh* 29-4. L370 is located at the end of the S4 domain; it represents the second leucine in the heptad repeat and is therefore referred to as L2. *Sh* channels with substitutions of other uncharged residues (G, A, S, C, T, V, P, I, M, F, or Y) at L370 (yielding G2, A2, etc., *Sh* proteins) were characterized by their effects on the gating and assembly of the expressed channels; charged and highly polar substitutions were not investigated because of the possible introduction of alterations in the electrostatic properties of the voltage sensor. We find that substitutions of L370 result in alterations in the relative stabilities of open, closed, and inactivated conformational states, corresponding to the size and hydrophobicity of the substituted residue. Furthermore, our data suggest that nonconservative substitutions of L370 influence the ability of *Sh* subunits to assemble into functional channel complexes. All of these observations are consistent with the idea that L370 and other residues in the region undergo protein interactions that are important determinants in the conformational structure of the channel.

MATERIALS AND METHODS

cDNA mutagenesis

Mutations were introduced into a modified form of the *Drosophila* Shaker 29-4 cDNA in Bluescript (Stratagene, La Jolla, CA). This modified 29-4 cDNA contains substitutions (TAGC) for nucleotides 1413–1416 (CTCA), yielding a silent mutation that introduces a novel *Sph*I site. Substitutions of L370 were introduced into the modified cDNA using the polymerase chain reaction with three different degenerate sense oligonucleotides that overlap a novel *Bsm*I site (nucleotides 1370–1376) and an antisense oligonucleotide that overlapped the novel *Sph*I site. Sense-strand oligonucleotides were partially degenerate for nucleotides 1384–1386 (TTA), the codon for leucine 370. The sequences of these oligonucleotides were

$$5'\text{-A TCT AGG CAT TCG AAG GGT } \begin{matrix}-\text{A}-\\ \text{GCT}\\ \text{TGC}\\ -\text{T}-\end{matrix} \text{ CAA ATA TTA GGA-3'} \quad \text{(A)}$$

$$5'\text{-A TCT AGG CAT TCG AAG GGT } \begin{matrix}-\text{A}-\\ \text{CCA}\\ \text{GG}-\end{matrix} \text{ CAA ATA TTA GGA-3'} \quad \text{(B)}$$

$$5'\text{-A TCT AGG CAT TCG AAG GGT ATA CAA ATA TTA GGA-3'}\\ -\text{CG} \quad \text{(C)}$$

and result in constructs that code, at position 370, for the following amino acid residues: (Oligo A) Ala, Asp, Cys, Gly, Phe, Ser, Tyr, and Val; (B) Ala, Arg, Gln, Glu, Gly, and Pro; (C) Ile, Met, and Thr. The polymerase chain reaction-generated fragments were restriction digested and cloned into the 29-4 cDNA using the novel *Bsm*I and *Sph*I restriction sites. Individual clones were identified by DNA sequencing with the Sequenase kit (US Biochemicals, Cleveland, OH) and sequencing was carried out until all of the potential mutations had been obtained except the charged or polar residue substitutions Arg, Asp, Gln, and Glu. As indicated, some of the constructs were truncated at the NH_2 terminus by deleting residues 2–30 to remove fast inactivation. In addition, for strongly expressing channel constructs, the cDNAs were put into a Bluescript vector containing a string of 40 adenosine nucleotides on the 3′ end of inserted cDNAs (the generous gift of R. Swanson).

Preparation of mRNA

Preparation of cDNA templates for synthesis of in vitro RNA transcripts was as follows: cDNA templates were digested with *Hind*III or, in the case of the polyA vector, *Not*I, incubated for 20 min with proteinase K (50 μg/ml) in 0.4% sodium dodecyl sulfate at 37°C, extracted twice with an equal volume of a 1:1 mixture of ether:chloroform, extracted once with ether, and then precipitated after the addition of 1/10 volume 3 M sodium acetate (pH 5.2) and 2.5 volumes of ethanol. Transcription reactions were carried out at 37°C in 40 mm Tris-Cl (pH 7.5); 6 mM $MgCl_2$; 2 mM spermidine (Sigma); 10 mM NaCl; 10 mM dithiothreitol (Sigma); 140 units human placental RNAse inhibitor (Promega); 0.5 mM diguanosine 5′-5′ triphosphate (pH 7.5, Pharmacia); 0.5 mM ATP, CTP, and UTP; 0.1 mM GTP (Pharmacia); 3 μg template cDNA; and 70 units of T7 RNA polymerase (Promega), in a total volume of 150 ml. After 2 h an additional 25 units of T7 polymerase was added to the reaction mixtures, which were incubated for another 3 h at 37°C. cDNA templates were then digested for 20 min at 37°C with 5 units DNAse I (RQ1; Promega). The reaction mixtures were then passed through G 50–80 Sephadex (Pharmacia) spun columns to remove unincorporated ribonucleoside triphosphates. RNA was extracted twice with a 1:1 mixture of phenol:chloroform and precipitated with a 1/10 volume of 3 M sodium acetate (pH 5.2) and 2.5 volumes of ethanol. The RNA was pelleted by centrifugation and then washed twice with 70% ethanol. Pellets were then air-dried, suspended in H_2O, and stored at −70°C.

Oocyte injection

Adult female *Xenopus laevis* were anesthetized in 0.14% 3-aminobenzoic ethyl ester (Sigma) for approximately 30 min, and a section of their ovaries surgically removed. Oocytes were dissociated by 2–3-h treatment with 2 mg/ml collagenase (type 1A; Sigma) in OR-3 (50% Liebovitz-15 medium; Gibco, Grand Island, NY), 50 units/ml Nystatin (Sigma), and 20 μg/ml Gentamicin (Sigma); washed four times with OR-3 medium; and placed at 18°C. One to three days later stage V and VI oocytes were injected with 50–70 nl of RNA and further incubated for 3–10 days at 18°C.

Electrophysiology

All experiments were carried out at room temperature (20–22°C). Two-microelectrode voltage clamp recordings were obtained with with an OC-725 voltage clamp (Warner Instruments) and the Acquire program (Instrutech Corp., Mineola, NY). Electrodes (0.3–0.7 MW resistance) were filled with 1 M KCl, and the oocytes were bathed in ND-96 (96 mM NaCl, 2 mM KCl, 1.8 mM $CaCl_2$, 1 mM $MgCl_2$, and 5 mM 4-(2-hydroxyethyl)-1-piperazineethanesulfonic acid (HEPES), pH 7.5). Data were filtered at 2 kHz.

For patch-clamp recordings, oocytes were placed in a hypertonic solution (0.2 M KAsp, 20 mM KCl, 10 mM EGTA, 1 mM $MgCl_2$, and 14 mM HEPES, pH 7.4) for 5–10 min prior to removal of the vitelline membrane with fine forceps. Patch pipettes were fabricated from Corning 7052 glass and were filled with either ND-96 or a solution containing 140 mM *N*-methyl-D-glucamine aspartate, 1 mM $CaCl_2$, and 10 mM HEPES (pH 7.4). Similarly, one of two bath solutions was used for cell-attached patches: ND-96 or a solution containing 138 mM KAsp, 2 mM KCl, 1 mM EGTA, 10 mM HEPES (pH 7.4). In the latter solution the resting potential of the oocytes is stabilized within a few millivolts of zero. Patch-clamp recordings were made using an EPC-9 amplifier (HEKA-Elektronik, Lambrecht, Germany) driven by the E9Acquire program. Data were filtered at 5 kHz (−3 db, Bessel response).

Electrophysiological data were analyzed using the Review program (Instrutech) and our own programs running in the PowerMod environment (HEKA). Linear leak and capacitive current were subtracted from the raw data by the P/4 procedure.

RESULTS

Effects on activation gating

Xenopus oocytes were injected with cRNAs encoding L2, G2, A2, S2, C2, T2, V2, P2, I2, M2, F2, or Y2 *Sh* proteins. Under two-microelectrode voltage clamp, most of the mutant channels produced large outward A-type currents similar to those of L2 channels (Fig. 2); upon depolarization they activate and then rapidly inactivate to various steady-state levels. However, all of the mutant channels activate at more positive potentials. The voltage dependence of peak conductance, a measure of channel activation, is plotted in Fig. 3 *A* for each channel type. Substitutions of larger hydropho-

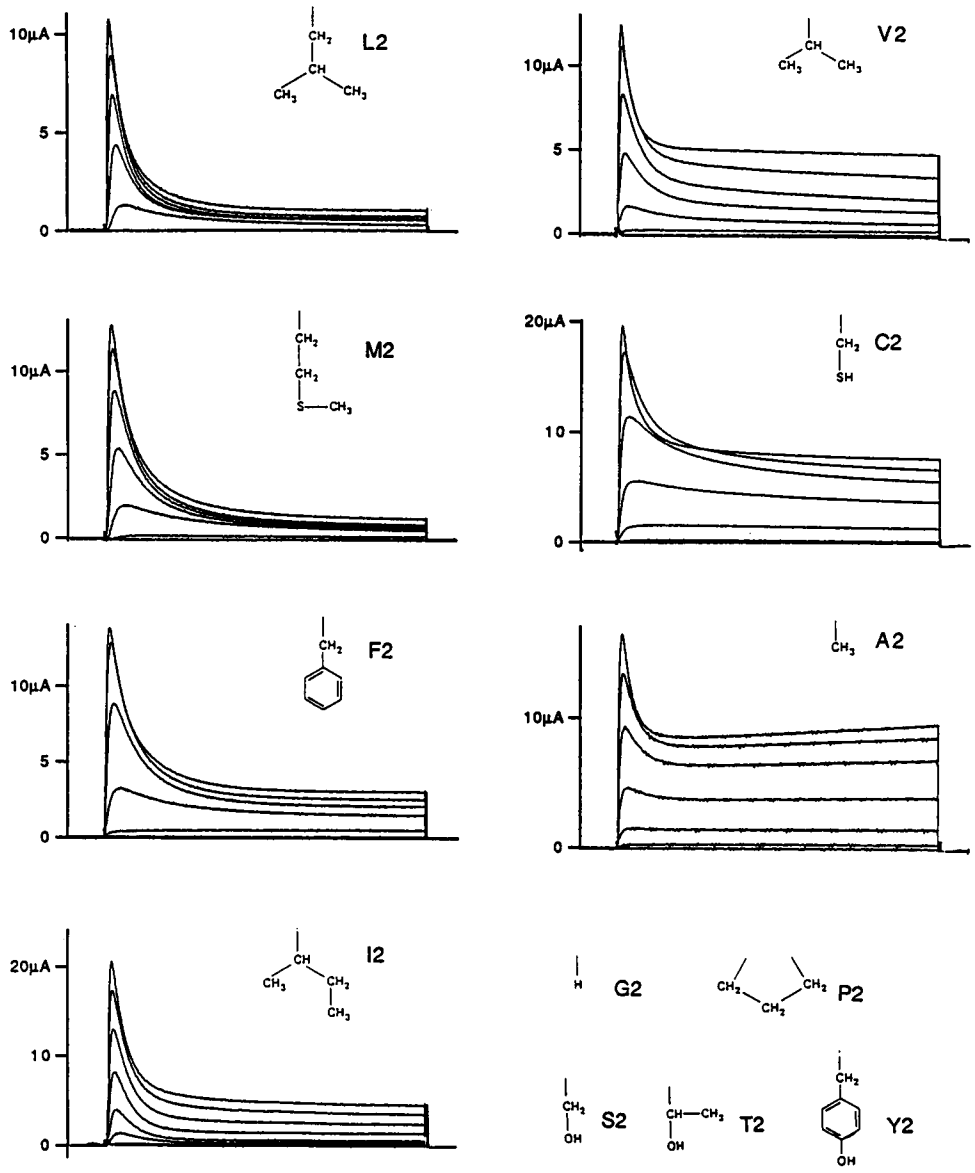

FIGURE 2 Whole-oocyte currents from *Sh* 29-4 channels substituted at amino acid position 370. Two-microelectrode voltage clamp recordings were made from *Xenopus* oocytes injected with L2 and the various mutant cRNAs. The current traces recorded for particular substitutions are indicated in letter code, and structural representations appear above the traces. Substitution mutations that did not express functional channels are listed at the bottom right. The membrane potential was held at −90 mV and depolarized to various voltages, in 20 mV increments, for 100 ms. The voltages (in mV) for the different substitutions were: L2, −40 to +80; M2, −40 to +80; F2, −20 to +100; I2, −20 to +120; V2, −20 to +120; C2, +20 to +140; A2, +60 to +180. Depolarizing pulses were given at 5-s intervals.

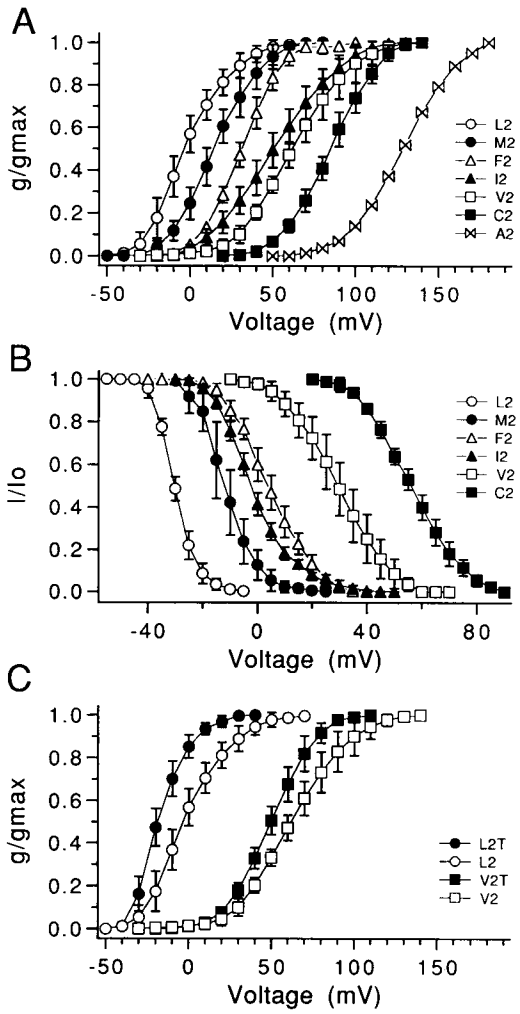

FIGURE 3 Voltage dependence of activation and inactivation for L370 substitution mutants. (*A*) normalized peak conductance as measured with 100-ms depolarizations from a holding potential of −90 mV. Conductance (g) was determined from $g = I_p/(V - V_k)$ where I_p is the peak current at voltage V, and the K^+ equilibrium potential V_k was taken to be −90 mV. The instantaneous I-V relationships could not be reliably measured in the voltage clamp, but patch clamp I-V relationships from L2 and V2 channels obtained under similar ionic conditions are essentially linear from −50 to +100 mV. Conductances were normalized by dividing the conductance at the indicated potential by the maximum conductance obtained. Currents were obtained after P/4 leak subtraction; the time between depolarizing pulses was 5 s (all constructs showed full recovery within this time period). Data are shown as mean ± SD, where n = 6, 7, 5, 9, 9, and 6 for L, M, F, I, V, and C constructs, respectively; for A2, data from a single oocyte having the largest expressed currents is shown. (*B*) normalized prepulse inactivation curves for the indicated channel constructs. From a holding potential of −100 mV, the membrane potential was stepped to the indicated prepulse voltages for 500 ms and then depolarized to a test potential chosen to give near-maximal peak conductance. The test potentials were +70 for L2, M2, and F2; +80 for I and V; and +120 for C. We were unable to obtain an inactivation curve for the A2 mutant because the large prepulse depolarizations at +160 mV, when applied for 500 ms, destroyed the oocyte membrane. Peak currents were normalized to the peak current obtained after a prepulse to −60 mV. Data are shown as mean ± SD, where n = 4, 5, 4, 3, 7, and 3 for L, M, F, I, V, and C, respectively. (*C*) normalized conductances of inactivating and noninactivating channels. The currents were obtained using a procedure identical to that described in (*A*). Data are mean ± SD, where n = 6, 5, 9, and 5 for L2, L2T, V2, and V2T constructs, respectively.

bic residues such as M shifted activation about 20 mV and produced small decreases in the slope of conductance-voltage relations, whereas substitutions of smaller residues such as A shifted activation to much higher depolarizing potentials and produced more significant decreases in slope. Prepulse inactivation curves of substituted channels are similarly shifted in the depolarizing direction and show a decrease in slope (Fig. 3 *B*). Less hydrophobic substitutions (G2, S2, T2, P2, and Y2) do not express measurable currents even at voltages up to +180 mV. Thus, larger and more hydrophobic residues substitute most efficiently for L370.

It is possible that some of the effects observed on activation gating are due to alterations in inactivation gating. Thus, we characterized WT, V2, I2, and A2 channels truncated at the NH_2 terminus (residues 2–30 were deleted), to abolish fast inactivation. Comparisons of activation between L2 and V2 channels and the corresponding truncated channels L2T and V2T are shown in Fig. 3 *C*. Although the presence of intact inactivation yields lower slopes of the peak conductance curves, it does not influence the conductance-voltage relations of the substituted channels more than the wild-type channel. This might be expected from the fact that the rates of inactivation for the different channel types is similar once the shifts in voltage dependence are accounted for (Table 1). Although there is evidence that Boltzmann fits of the activation and inactivation curves do not accurately reflect the valence of the gating charge z of *Sh* channels (Schoppa et al., 1992), we quantified the voltage dependence of channel opening through Boltzmann fits to the inactivation curves for the different mutant channels for comparison (Table 1). This z value decreases with increasing inactivation midpoint voltage V_h in the various functional channel types.

Two-microelectrode recordings of oocytes injected with "high expressing" L2T, V2T, A2T, and G2T polyadenylated RNA constructs are shown in Fig. 4. For constructs that express ionic currents (L2T, V2T, and A2T) gating currents can be easily measured up to threshold potentials of channel activation without the use of channel blockers (no gating currents are observed for L370-substituted channels that do not express measurable ionic currents, e.g., G2T; see below). Although complete charge movement (Q)-voltage relations cannot be determined for the channels above activating potentials, for the A2T channels it appears that the charge movement reaches a plateau well below 0 mV, and only small increases in Q are observed over the range of potentials where the channels begin to open, $\geq$ +20 mV. Thus, as previously observed in a patch-clamp study of V2T channels (Schoppa et al., 1992), the actual opening step of A2T channels appears to be associated with a relatively small component of the gating charge movement. The similarities between the A2T and V2T gating currents is consistent with the idea that the graded effects of the various substitutions reflect a common mechanism that underlies both the voltage shifts and the decreases in slope.

TABLE 1 Properties of L370 substitution mutants

Sh cDNA	V_m	*n*	V_h	*z*	*n*	τ_1	τ_2	A1	A2	I_{ss}	*n*
L2	−1 ± 5.6	6	−30 ± 0.9	6.41 ± 0.7	4	5.6 ± 0.81	20 ± 4	0.60 ± 0.06	0.25 ± 0.04	0.14 ± 0.08	5
M2	15 ± 5.3	7	−11 ± 3.0	4.75 ± 0.5	5	5.9 ± 0.85	18 ± 3	0.51 ± 0.11	0.34 ± 0.10	0.16 ± 0.07	6
F2	31 ± 2.9	5	4 ± 2.5	3.18 ± 0.1	4	5.8 ± 1.4	17 ± 5	0.47 ± 0.09	0.29 ± 0.11	0.24 ± 0.12	5
12	52 ± 6.7	9	−2 ± 1.4	3.46 ± 0.4	3	4.4 ± 0.44	26 ± 8	0.72 ± 0.04	0.07 ± 0.05	0.22 ± 0.03	8
V2	64 ± 6.8	4	28 ± 5.7	2.84 ± 0.2	8	5.6 ± 0.62	39 ± 10	0.57 ± 0.04	0.15 ± 0.05	0.28 ± 0.07	7
C2	85 ± 3.9	6	56 ± 1.9	2.83 ± 0.3	3	8.5 ± 1.9	47 ± 13	0.29 ± 0.04	0.23 ± 0.09	0.49 ± 0.07	6
A2	128	1									

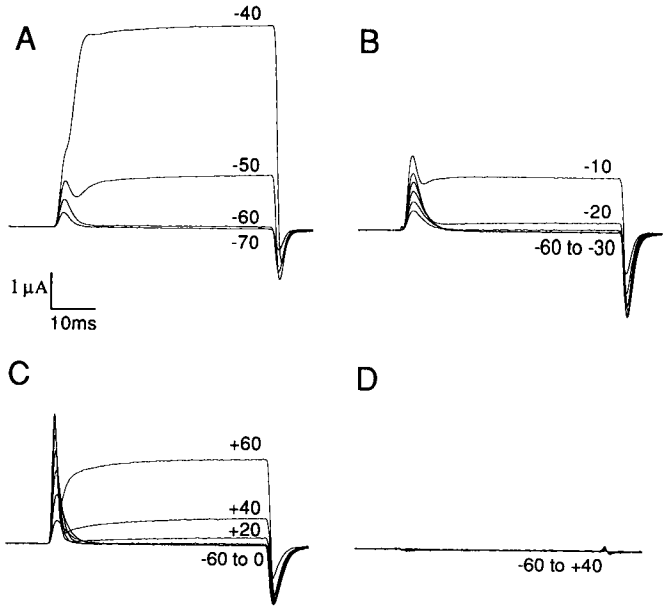

FIGURE 4 Gating and ionic currents of *Sh* constructs measured with the two-microelectrode voltage clamp. (*A*) L2T channels; (*B*) V2T channels; (*C*) A2T channels; (*D*) G2T channels. Oocyte membranes were held at −100 mV and then depolarized to the indicated potentials for 50 ms. The potentials used were picked for the indicated constructs in order to show the range of gating currents prior to channel opening as well as the ionic currents at low open probability. The on gating currents peak within a few milliseconds at the beginning of each depolarizing pulse, and the off currents peak when brought back to the holding potential of −100 mV. The slower noninactivating ionic currents can be seen as the plateau levels in the current traces during the depolarizing pulses. Currents in response to depolarizing pulses in 10-mV increments are shown for L2T and V2T channels and in 20-mV increments for A2T and G2T channels. The traces are averages of 4 sweeps taken at 5-s intervals as obtained after leakage subtraction using scaled, alternating-polarity pulses of 10 mV from a holding potential of −110 mV. The small unsubtracted artifact observed in G2T cRNA-injected oocytes was identical to that of control uninjected oocytes (not shown).

Effects on inactivation

Sh 29-4 channels exhibit a double exponential inactivation (Iverson and Rudy, 1990); the amplitude A_1 of the fast component is larger, roughly twice the amplitude A_2 of the slower component (Table 1). Unfortunately, the details of this process are not well understood in comparison to the inactivation of another *Sh* splice product, *Sh* B. The latter contains a different NH_2 terminus, shows single exponential fast inactivation, and is thought to inactivate through the binding of the NH_2-terminal "ball" to a receptor site at the internal mouth of the pore (Hoshi et al., 1990). Although both types of *Sh* products are susceptible to a slower C-type inactivation (Iverson and Rudy, 1990), it can be ignored over the 100-ms pulses we have used. In addition, in 29-4 channels there remains a substantial component of "steady-state" current (I_{ss}) remaining at the end of 100-ms pulses.

Interestingly, each of the L370 mutations has larger I_{ss} values than the wild type. The fraction of steady-state current measured near maximally activating potentials shows a systematic increase with shifts in V_h, increasing in value from about 14% in L2 to about 50% or greater in the mutants C2 and A2, which had the largest shifts (see Table 1 and Fig. 2). The increasing I_{ss} suggests that substitutions at this position not only destabilize the open state relative to closed states but that they also result in a corresponding destabilization of the inactivated state relative to the open state.

We were concerned about possible artifactual origins of the steady-state current. A slowly activating outward current endogenous to the oocytes probably contributes to the currents at the highest depolarizations, for example, in the C2 and A2 traces at +140 to +180 mV shown in Fig. 2. However, the steady-state current levels observed in L2-injected oocytes at these potentials never approach the level observed for the mutant channels. This is true even at potentials where the peak conductance of a mutant channel is nearly saturated and has inactivation rates similar to those of L2; for example, compare L2 and V2 currents at +80 mV (Fig. 2). Uncompensated series resistance (R_s) tends to slow the time course of inactivation and increase the apparent I_{ss} when the expressed channel current is large. Measurements of R_s in our setup, obtained by applying current pulses to the cell, gave relatively low values, in the range of 100–200 W, but invaginations of the membrane may cause a substantial fraction of the membrane area to have a higher access resistance.

In an attempt to determine the origin of the increased I_{ss} in the mutant channels, we obtained macro-patch recordings from oocytes expressing L2 and V2 channels. Recordings were first made using an *N*-methyl-D-glucamine solution in the pipette and a K-aspartate depolarizing solution in the bath. Cell-attached recordings (Fig. 5, *A* and *C*) showed more complete inactivation in both L2 and V2 channels than observed in the whole-oocyte recordings, but I_{ss} continued to be larger in V2. Upon excision to form inside-out patches, I_{ss} generally decreased even further (Fig. 5, *B* and *D*). Similar increases in I_{ss}, corresponding to the extent of the voltage shift, were observed for the other L370-substituted channels (data not shown).

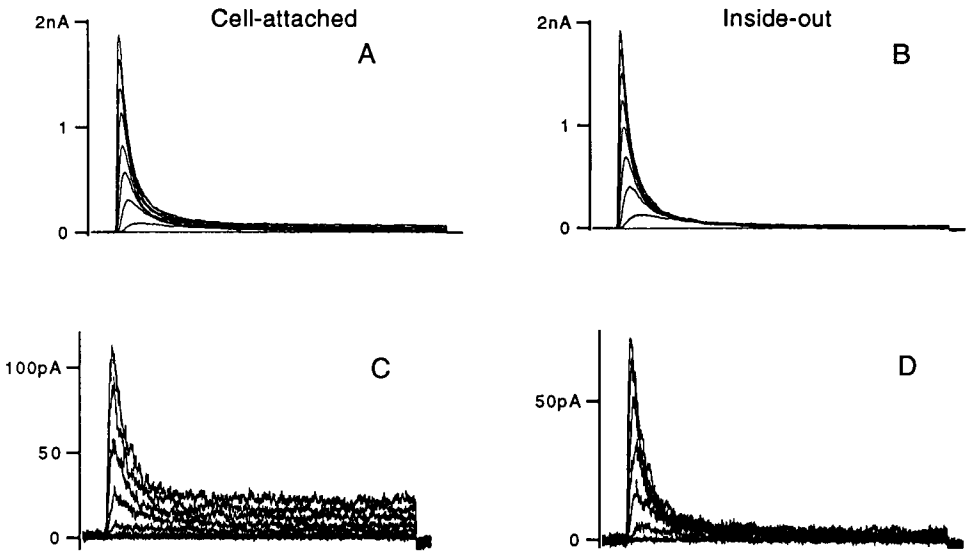

FIGURE 5 Macropatch recordings of L2 and V2 channels in cell-attached and inside-out configurations. Patch pipettes were fabricated with 1–2-mm-diameter tips and filled with 140 mM *N*-methyl-D-glucamine solution (see Materials and Methods). The bath solution was 138 mM KAsp. Patches were held at −90 mV and depolarized at 5-s intervals. Each trace is the average of three sweeps. (*A*) currents from a cell-attached patch of L2 channels at depolarizations from −60 to +120 mV in steps of 20 mV. (*B*) the same L2 patch at the same potentials, but after excision to form the inside-out configuration. (*C*) a cell-attached patch of V2 at potentials from 0 to +120 mV in steps of 20 mV. (*D*) recordings from the same V2 patch after excision.

Since the discrepancy between whole-oocyte and cell-attached recordings could result from the different solutions bathing the membrane, we then obtained cell-attached recordings using the same ND-96 solution in the pipette and bath that was used in the whole-oocyte recordings. Again, however, I_{ss} was about half as large in the cell-attached patch recordings. While the differences in I_{ss} between patch and whole-oocyte recordings remain unexplained (and I_{ss} is quite variable in each recording configuration), it is always larger on average by a factor of 2 to 3 in V2 channels than in L2 channels. This is in agreement with single channel studies where V2 channels were observed to reopen more frequently from inactivated states (McCormack et al., 1991) and the idea that mutations of L370 do decrease the relative stability of the inactivated state of the channel. This presents two possibilities for the effects on inactivation resulting from substitutions at L370: (*a*) L370 is involved directly in the binding of the inactivation ball or (*b*) substitutions of L370 indirectly alter the structure of the ball receptor site or the stability of the inactivated state.

Role in subunit assembly

Although six of the mutant channels described here are altered in their gating properties, we were unable to obtain expression of the five other mutant channel types, G2, S2, T2, P2, and Y2. There are two simple explanations for the nonexpression of the channels: (*a*) they shift activation to immeasurably large positive potentials or (*b*) they do not assemble into tetrameric complexes.

To test these possibilities we attempted to form hybrid channels, as have been previously observed with the coinjection of wild-type and V2 cRNAs (McCormack et al., 1990). Mutant cRNAs and cRNA from a truncated L2 construct (L2T) were coinjected in a 3:1 ratio (Fig. 6). This ratio was chosen because we find that NH_2-terminal truncated cRNAs express approximately threefold more peak current than nontruncated channel cRNAs, perhaps because the truncated construct lacks all but the last 10 nucleotides of the untranslated 5′ sequence. When coinjected with G2, P2, or Y2, an inactivating current component appeared that showed prepulse inactivation at potentials 20–30 mV more positive than those observed in L2 (Fig. 5). Thus, some of the inactivating mutant subunits are incorporated with wild-type subunits to yield inactivating channels with shifted voltage dependence.

Since the homotetramer activation voltages of the G2, P2, or Y2 subunits would have to be shifted to potentials so large that their currents cannot be detected (greater than +180 mV), larger shifts would be expected to arise if more than one of these subunits were contained in the channel complex (McCormack et al., 1990, 1992; Tytgat and Hess, 1992). Thus the data suggest that only one of these mutant subunits can be incorporated into a functional channel. When more than one is incorporated it would appear to result in a nonfunctional channel or to inhibit the assembly process; consistent with this idea is the fact that the magnitude of the coinjected currents was roughly one-fourth the magnitude of those obtained from L2T cRNA alone. In one set of experiments the currents generated by approximately 3 ng of injected L2T RNA and 40-mV depolarizations was 35.5 ± 11 mA (mean ± SD, n = 4), whereas coinjection of L2T and G2 (3 and 9 ng, respectively) yielded 7.7 ± 3 mA (mean ± SD, n = 4). Only small differences were seen in the voltage dependence of activation upon addition of the G2 RNA. Similar coinjections of T2 or S2 with L2T cRNA resulted in currents having prepulse inactivation that was nearly indistinguishable from that of the L2T construct alone. Moreover, the coinjection of S2 and T2 with L2T RNA showed less suppression of the noninactivating L2T currents (about twofold), suggesting that S2 and T2 subunits may coassemble even more poorly than G2, P2, and Y2 subunits. In the same batch of oocytes coinjections of L2T (3 ng) and T2 or S2 (9 ng) produced 14.1 ± 8.8 mA (mean ± SD, n = 4) or 18.7 ± 6.7 mA (mean ± SD, n = 5), respectively. As a

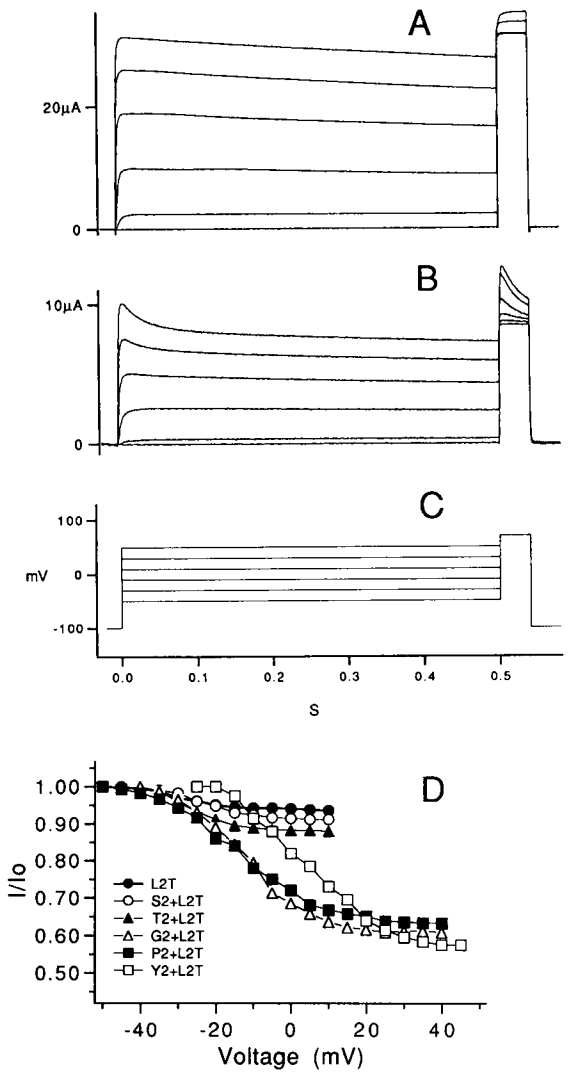

FIGURE 6 Expression of currents from L2T alone (*A*) and coinjection of G2 and L2T (*B*). (*C*) voltage protocol. Prepulse depolarizations (500 ms) were applied to potentials from −50 mV to +50 mV in steps of 20 mV; these were followed by a test pulse at +70 mV. L2T channels showed little inactivation during the 500-ms prepulses, while the coinjected cRNAs resulted in a small, rapidly inactivating component. (*D*) prepulse inactivation curves for coinjected currents. The normalized peak current during the +70 mV test pulse is plotted as a function of the prepulse potential. L2T and the coinjections S2 + L2T and T2 + L2T showed only the slight inactivation expected from the slow process that is visible in (*A*). G2 + L2T, P2 + L2T, and Y2 + L2T showed an additional inactivating current component with apparent midpoint voltages V_h near −10 to 0 mV.

further test for the assembly of these mutants we measured the gating currents from oocytes injected with truncated and polyadenylated G2, P2, and Y2 constructs (G2T, P2T, and Y2T) identical to those used for L2, V2, and A2. Unlike the V2T and A2T channels, no detectable gating currents were observed for G2T (Fig. 4 *A*), P2T, or Y2T channels. This suggests that these mutant subunits do not assemble into tetrameric complexes or that in contrast to the other mutations, they shift gating charge movement to extremely high potentials.

DISCUSSION

Substitution effects on gating

Every amino acid residue substituted for L2 causes a shift in the channel activation to more depolarizing potentials. Moreover, the magnitudes of the voltage shifts corresponded with (*a*) the degree of the decrease in the slopes of the peak conductance-voltage (Fig. 3 *A*) and prepulse inactivation curves (Fig. 3 *B* and Table 1) and (*b*) the increase in I_{ss} levels (Fig. 2 and Table 1).

In proteins with known structure, residues that are buried and interact with other residues in the protein are usually hydrophobic and well conserved, while those that interact with solvent, whether aqueous or lipid, are poorly conserved (Go and Miyazawa, 1980; Rees et al., 1989). In addition, the substitution of buried residues in other proteins has revealed three principal determinants that influence the side-chain interactions of these residues: hydrophobicity, volume, and steric complementarity (Bowie et al., 1990; Eriksson et al., 1992; Mendel et al., 1992). The rank order of substitution effects observed for L370,

$$L < M < F < I < V < C < A < G, P, Y, T, \text{and } S, \quad \text{(I)}$$

differs in detail from the hydrophobicity sequence of amino acid residues according to Engelman et al. (1986),

$$F < M < I < L < V < C < A < T < G < S < P < Y, \quad \text{(II)}$$

obtained from the relative free energy of transfer for these residues in α-helix between aqueous and nonpolar environments. Thus, other factors are likely to play a role in the interactions of L370. Substitutions of buried leucine residues in other proteins has shown that smaller residues, such as alanine, induce cavities that reduce conformational stability (Eriksson et al., 1992; Mendel et al., 1992). In leucine zipper proteins steric complementarity plays a critical role in the packing of leucine residues. In the structure of GCN4, leucines in the heptad repeat are seen to pack very efficiently with hydrophobic residues in the adjacent helical strand (O'Shea et al., 1991). The idea that L370 undergoes interactions with similar structural requirements is consistent with a study of the dimerization of C/EBP (Landschulz et al., 1989) which showed that substitutions of a single leucine residue, the second in the heptad repeat, reduce the stability of the dimeric form in the order

$$L < M < I < V, \quad \text{(III)}$$

which is identical to the ranking that we observe. Thus, L370 is likely to be at least partially buried in hydrophobic interactions in conformational states close to channel opening.

As observed here, substitutions of L2 result in a positive shift in the voltage dependence of activation, that is, toward a reduction in channel open probability at a given potential. Less conservative substitutions, with respect to hydrophobicity, size, and steric complementarity, result in larger shifts. Because larger and more hydrophobic residues (e.g., M or F)

substitute better than smaller residues (e.g., A) it suggests that the residue 370 side chain undergoes relatively specific interactions. These effects contrast with those expected when it is assumed that the gating alterations, resulting from the substitutions, take place primarily through the introduction of steric constraints on S4 movement since substitution with other large residues might be expected to introduce the greatest steric interference (Auld et al., 1990). Thus, the simplest explanation for the graded effects of the various substitutions is that they reflect varying levels of perturbation of the intraprotein interactions of L370 and that these interactions are critical to the stability of the open state of the channel.

Inactivation gating

It is curious that the increases in I_{ss} levels during two-microelectrode recordings correlate so well with the degree of voltage shift and slope changes in the various mutations. Elevated I_{ss} values were also seen with macropatch recordings from mutant channels, although the magnitudes of I_{ss} found using this technique were smaller. If L370 interacts directly with the NH_2-terminal inactivating region (Hoshi et al., 1990), one would have to explain this correlation by suggesting that the interaction between L370 and the ball is affected with exactly the same specificity as that found for the interactions of L370 during activation. On the other hand it is possible that L370 does not interact directly with the inactivation ball. The alterations in I_{ss} could be due to alterations in the relative stabilities of the open and inactivated closed conformational states or indirect alterations in the ball receptor site.

From the data at hand it seems more likely that the effects of L370 on I_{ss} levels are not due to direct interaction with the inactivation ball for three reasons: (*a*) increases in I_{ss} correspond with the degree of the voltage shifts and slope decreases in the L370 mutations; (*b*) residue 370 is likely to be at least partially buried within hydrophobic contacts and unable to interact with an inactivation ball during the later stages of channel gating and probably during channel opening; (*c*) increases in steady-state current have been seen in the past in oocyte voltage-clamp recordings of *Sh* channel mutants well into the S4 domain. Current recordings of the V1 mutation (L363V in *Sh* 29-4) (McCormack et al., 1991) and those presented for the *Sh*B S4 charged-residue mutations that also induce positive shifts in channel activation also show increased I_{ss} levels (Papazian et al., 1991). Thus increases in I_{ss} may generally result from mutations that cause depolarizing activation and inactivation shifts. Moreover, unless the major portion of the S4 domain is exposed to the cytoplasmic surface of the membrane to form part of the ball receptor during channel opening, one expects that these I_{ss} changes are mediated by indirect effects on the structure or stability of the ball receptor site. The data therefore suggest that L370 is unlikely to be involved directly in forming the ball receptor site. Whether a larger region between S4 and S5 determines this site and a portion of the internal mouth of the pore (Isacoff et al., 1991) remains to be shown.

Changes in the ΔG of channel activation

In the context of the model of Schoppa et al. (1989), one can estimate the perturbation due to amino acid substitution, of the free energy change ΔG accompanying channel opening; the transition that is most perturbed has a charge movement $q = 2.3$ elementary charges, and the V2 mutation shifts the midpoint voltage of this transition by $\Delta V = 63$ mV, corresponding to a free energy change of

$$\Delta\Delta G = q\Delta V$$

or 3.5 kcal/mol. The ΔV for A2 is about 130 mV, yielding $\Delta\Delta G \approx 7$ kcal/mol, and the small ΔV of 16 mV for M2 corresponds to $\Delta\Delta G = 0.9$ kcal/mol. If we assume that the energetic contribution of each subunit to the conformational change is additive, one finds the resulting free energy changes, ranging from about 0.2 to 2 kcal/mol, to be of the correct order of magnitude for the transfer of the side chain from a relatively polar environment to a hydrophobic one during channel activation. It remains possible, however, that the effects of these mutations are not additive among subunits; *Sh* subunits may gate cooperatively (Stühmer et al., 1991; Tytgat and Hess, 1992), and residues in the heptad repeat may mediate or influence such interactions (McCormack et al., 1989, 1991).

Assembly

Not only is the activation and inactivation gating of *Sh* altered by the substitutions at L370, but it appears that the less conservatively mutated subunits (G, P, Y, T, and S) are unlikely to form tetrameric channel complexes. At least a partial assembly is indicated for these subunits because of the decreases in magnitude of the coinjected L2T channel currents; such decreases probably take place through the association of the mutated and L2T subunits in an NH_2-terminal subunit association region whereby mutated subunits can bind and sequester some of the L2T subunits from the pool of functional subunits (McCormack et al., 1991, 1992; Li et al., 1992). In agreement with this idea is the fact that coinjections either produce a relatively small shift in the voltage dependence (G2, P2, and Y2), consistent with only one mutant subunit per functional tetramer, or they have no effect on the L2T gating properties (T2 and S2), as though they do not form functional hybrid tetramers at all. In addition, no detectable gating charge movement is observed for the homotetrameric channels G2T, P2T, and Y2T, and the majority of gating charge movement for the functional mutants V2T and A2T moves at potentials similar to that of wild-type channels. The simplest explanation for the data is that the G, P, Y, T, and S substitutions inhibit the ability of the subunits to assemble into tetrameric complexes.

Increasingly smaller and less hydrophobic residues appear to produce correspondingly greater alterations in the acti-

vation, inactivation, and assembly of *Sh* channels. This indicates that L370 is involved in specific protein interactions that play a critical role in determining the conformational stability of *Sh*. Moreover, because our data suggest that substitutions of L370 affect both activation and assembly, this residue may play similar roles during these processes, which is consistent with the idea that the S4 domain undergoes a large translocation in the membrane during activation as well as during the folding or insertion processes of channel assembly.

We are grateful to L. E. Iverson and M. A. Tanouye, in whose laboratories much of the molecular work for this study was done, and to W. Stühmer, in whose laboratory some of the physiology experiments were completed. Thanks also go to S. H. Heinemann, R. Ayer, A. Parekh, N. Schoppa, and M. Hoth for their comments in the preparation of the manuscript.
This work was supported by NIH grant NS21501 to F. J. S. K. M. was supported by NIH training grant NS07102 and a long-term HFSP fellowship.

REFERENCES

Abel, T., and T. Maniatis. 1989. Action of leucine zippers. *Nature (Lond.).* 341:24–25.

Auld, V. J., A. L. Goldin, D. S. Krafte, W. Catterall, H. A. Lester, N. Davidson, and R. Dunn. 1990. A neutral amino acid change in segment IIS4 dramatically alters the gating properties of the voltage-dependent sodium channel. *Proc. Natl. Acad. Sci. USA.* 87:323–327.

Bezanilla, F., E. Perozo, D. M. Papayian, and E. Stefani. 1991. Molecular basis of gating charge immobilization in Shaker potassium channels. *Science (Washington DC).* 254:679–683.

Bowie, J. U., J. F. Reidhaar-Olson, W. A. Lim, and R. T. Sauer. 1990. Deciphering the message in protein sequences: tolerance to amino acid substitutions. *Science (Washington DC).* 247:1306–1310.

Butler, A., A. Wei, K. Baker, and L. Salkoff. 1990. A family of putative potassium channel genes in *Drosophila*. *Science (Washington DC).* 243: 943–947.

Catterall, W. A. 1988. Structure and function of voltage-sensitive ion channels. *Science (Washington DC).* 242:50–60.

Engelman, D. M., T. A. Steitz, and A. Goldman, A. 1986. Identifying nonpolar transbilayer helices in amino acid sequence4s of membrane proteins. *Annu. Rev. Biohys. Chem.* 15:321–353.

Eriksson, A. E., W. A. Baase, X-J. Zhang, D. W. Heinz, M. Blaber, E. P. Baldwin, and B. W. Matthews. 1992. Response of a protein structure to cavity-creating mutations and its relation to the hydrophobic effect. *Science (Washington DC)* 255:178–183.

Go, M., and S. Miyazawa. 1980. Relationship between mutability, polarity and exteriority of amino acid residues in protein evolution. *Int. J. Pept. Protein Res.* 15:211–224.

Hartmann, H. A., G. E. Kirsch, M. Drewe, R. H. Taglialatella, Joho, and A. M. Brown. 1991. Exchange of conduction pathways between two related K^+ channels. *Science (Washington DC).* 251:942–944.

Hoshi, T., W. N. Zagotta, and R. W. Aldrich. 1990. Biophysical and molecular mechanisms of Shaker potassium channel inactivation. *Science (Washington DC).* 250:533–538.

Isacoff, E. Y., Y. N. Jan, and L. Y. N. Jan. 1991. Putative receptor for the cytoplasmic inactivation gate in the Shaker K^+ channel. *Nature (Lond.).* 353:86–90.

Iverson, L. E., and B. Rudy. 1990. The role of divergent amino and carboxyl domains on the inactivation properties of potassium channels derived from the Shaker gene of *Drosophila*. *J. Neurosci.* 10:2903–2916.

Landschulz, W. H., P. F. Johnson, and S. L. McKnight. 1989. The DNA binding domain of the rat liver nuclear protein C/EBP is bipartite. *Science (Washington DC).* 243:1681–1688.

Li, M., L. Y. Jan, and Y. N. Jan. 1992. Specification of subunit assembly by the hydrophilic amino-terminal domain of the Shaker potassium channel. *Science (Washington DC).* 257:1225–1230.

Liman, E. R., P. Hess, F. Weaver, and G. Koren. 1991. Voltage-sensing residues in the S4 region of a mammalian K^+ channel. *Nature (Lond.).* 353:752–756.

Liman, E., J. Tytgat, and P. Hess. 1992. Subunit stoichiometry of a mammalian K^+ channel determined by the construction of mutimeric cDNAs. *Neuron.* 9:861–871.

Logothetis, D. E., S. Movahedi, C. Satler, K. Lindpaintner, and B. Nadal-Ginard. 1992. Incremental reductions of positive charge within the S4 region of a voltage-gated K^+ channel result in corresponding decreases in gating charge. *Neuron.* 8:531–540.

MacKinnon, R. 1991. Determination of the subunits stoichiometry of a voltage-activated potassium channel. *Nature (Lond.).* 350:232–235.

McCormack, K., J. T. Campanelli, M. Ramaswami, M. K. Mathew, M. A. Tanouye, L. E. Iverson, and B. Rudy. 1989. Leucine zipper motif update. *Nature (Lond.).* 340:103.

McCormack, K., J. W. Lin, L. E. Iverson, and B. Rudy. 1990. Shaker K^+ channel subunits form heteromultimeric channels with novel functional properties. *Biochem. Biophys. Res. Commun.* 171:1361–1371.

McCormack, K., M. A. Tanouye, L. E. Iverson, J. W. Lin, M. Ramaswami, T. McCormack, J. T. Campanelli, M. K. Mathew, and B. Rudy. 1991. A role for hydrophobic residues in the voltage-dependent gating of Shaker K^+ channels. *Proc. Natl. Acad. Sci. USA.* 88:2931–2935.

McCormack, K., L. Lin, L. E. Iverson, M. A. Tanouye, and F. J. Sigworth. 1992. Tandem linkage of Shaker K^+ channel subunits does not ensure the stoichiometry of expressed channels. *Biophys. J.* 63:1406–1411.

Mendel, D., J. A. Ellman, Z. Chang, D. L. Veenstra, P. A. Kollman, and P. G. Schultz. 1992. Probing protein stability with unnatural amino acids. *Science (Washington DC).* 256:1798–1802.

Noda, M., T. Ikeda, T. Kayano, H. Suzuki, H. Takeshima, M. Kurasaki, H. Takahashi, and S. Numa. 1986. Existence of distinct sodium chanel messenger RNAs in rat brain. *Nature (Lond.).* 320:188–192.

O'Shea, E. K., J. D. Klemm, P. S. Kim, and T. Alber. 1991. X-ray structure of the GCN4 leucine zipper, a two-stranded, parallel coiled-coil. *Science (Washington DC).* 254:539–544.

Papazian, D. M., L. C. Timpe, Y. N. Jan, and L. Y. Jan. 1991. Alteration of voltage-dependence of Shaker potassium channel by mutations in the S4 sequence. *Nature (Lond.).* 349:305–310.

Rees, D. C., L. DeAntonio, and D. Eisenberg. 1989. Hydrophobic organization of membrane proteins. *Science (Washington DC).* 245:510–513.

Schoppa, N., K. McCormack, M. A. Tanouye, and F. J. Sigworth. 1992. Size of gating charge in wild type and mutant Shaker potassium channels. *Science (Washington DC).* 255:1712–1715.

Stühmer, W., F. Conti, H. Suzuki, X. Wang, M. Noda, N. Yahagi, H. Kubo, and S. Numa. 1989. Structural parts involved in activation and inactivation of the sodium channel. *Nature (Lond.).* 339:597–603.

Stühmer, W., F. Conti, M. Stocker, O. Pongs, and S. H. Heinemann. 1991. Gating currents of inactivating and noninactivating potassium channels expressed in *Xenopus* oocytes. *Pflügers Arch. Eur. J. Physiol.* 418:423–429.

Tanabe, T., H. Takeshima, A. Mikami, V. Flockerzi, H. Takahashi, K. Kangawa, M. Kojima, H. Matsuo, T. Hirose, and S. Numa. 1987. Primary structure of the receptor for calcium channel blockers form skeletal muscle. *Nature (Lond.).* 328:313–318.

Tempel, B., D. M. Papazian, T. L. Schwarz, Y. N. Jan, and L. Y. Jan. 1987. Sequence of a probable potassium channel component encoded at the Shaker locus of *Drosophila*. *Science (Washington DC).* 237:770–775.

Tytgat, J., and P. Hess. 1992. Evidence for cooperative interactions in potassium channel gating. *Nature (Lond.).* 359:420–423.

Yellen, G. M., M. E. Jurman, T. Abramson, and R. MacKinnon. 1991. Mutations affecting internal TEA blockade identify the probable pore-forming region of a K+ channel. *Science (Washington DC).* 251:939–942.

Yool, A. J., and T. L. Schwarz. 1991. Alteration of ionic selectivity of a K^+ channel by mutation of the H5 region. *Nature (Lond.).* 349:700–704.